Extending Sommerfeld integral based spherical wavefield computations beyond two layers

Arnim B. Haase
CREWES, University of Calgary

CREWES

Outline

- Introduction
- Sommerfeld Integrals and seismic wave fields
- Point sources in layered half spaces: Ewing, Jardetzky and Press
- Interfaces and boundary conditions
- P-wave multiples in a three-layer system
- Class 1 AVO-response of a three-layer system
- Conclusions
- Acknowledgements

$$u_P(\omega) = i\omega e^{-i\omega t}\int_0^\infty \left[\frac{p^2}{\xi} J_1(\omega pr)\sin(\theta) - ipJ_0(\omega pr)\cos(\theta)\right] e^{i\omega z\xi}\, dp$$

Direct-Wave Particle Motion Based on Sommerfeld Integral (Aki and Richards, 1980)

$$\varphi_j = \int_0^\infty Q_j^{'} J_0(kr) e^{-\nu_j z} dk + \int_0^\infty Q_j^{''} J_0(kr) e^{\nu_j z} dk$$

$$\psi_j = \int_0^\infty S_j^{'} J_0(kr) e^{-\nu_j^{'} z} dk + \int_0^\infty S_j^{''} J_0(kr) e^{\nu_j^{'} z} dk$$

Potential of Down-Going and Up-Going Waves in Layer *j* (Ewing, Jardetzky and Press, 1957)

$$A_{R1}\alpha_1 p + B_{R1}\beta_1\eta_1 - (A_{T1} + A_{R2}e^{-i\omega\xi_2 z_2})\alpha_2 p - (B_{T1} + B_{R2}e^{-i\omega\eta_2 z_2})\beta_2\eta_2 = -A_{I1}\alpha_1 p$$

$$-A_{R1}\alpha_1\xi_1 + B_{R1}\beta_1 p - (A_{T1} - A_{R2}e^{-i\omega\xi_2 z_2})\alpha_2\xi_2 + (B_{T1} - B_{R2}e^{-i\omega\eta_2 z_2})\beta_2 p = -A_{I1}\alpha_1\xi_1$$

$$-2A_{R1}\alpha_1\beta_1^2\rho_1 p\xi_1 - B_{R1}\beta_1\rho_1(1-2\beta_1^2 p^2) - (A_{T1} - A_{R2}e^{-i\omega\xi_2 z_2})2\alpha_2\beta_2^2\rho_2 p\xi_2$$
$$-(B_{T1} - B_{R2}e^{-i\omega\eta_2 z_2})\beta_2\rho_2(1-2\beta_2^2 p^2) = -2A_{I1}\alpha_1\beta_1^2\rho_1 p\xi_1$$

$$A_{R1}\alpha_1\rho_1(1-2\beta_1^2 p^2) - 2B_{R1}\beta_1^3\rho_1 p\eta_1 - (A_{T1} + A_{R2}e^{-i\omega\xi_2 z_2})\alpha_2\rho_2(1-2\beta_2^2 p^2)$$
$$+(B_{T1} + B_{R2}e^{-i\omega\eta_2 z_2})2\beta_2^3\rho_2 p\eta_2 = -A_{I1}\alpha_1\rho_1(1-2\beta_1^2 p^2)$$

Application of Boundary Conditions at the First Interface ($z_1 = 0$)

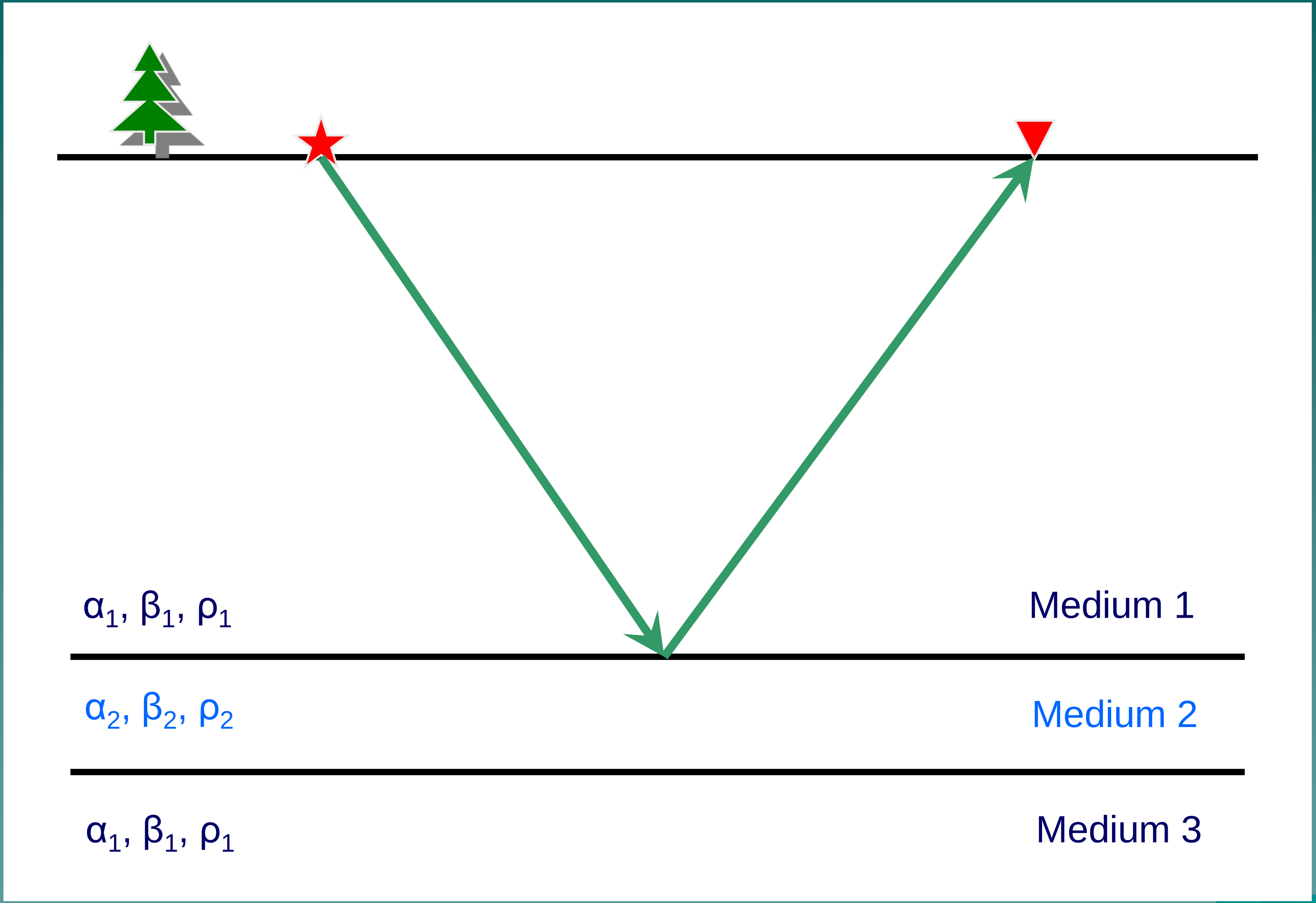

Reservoir Model Geometry

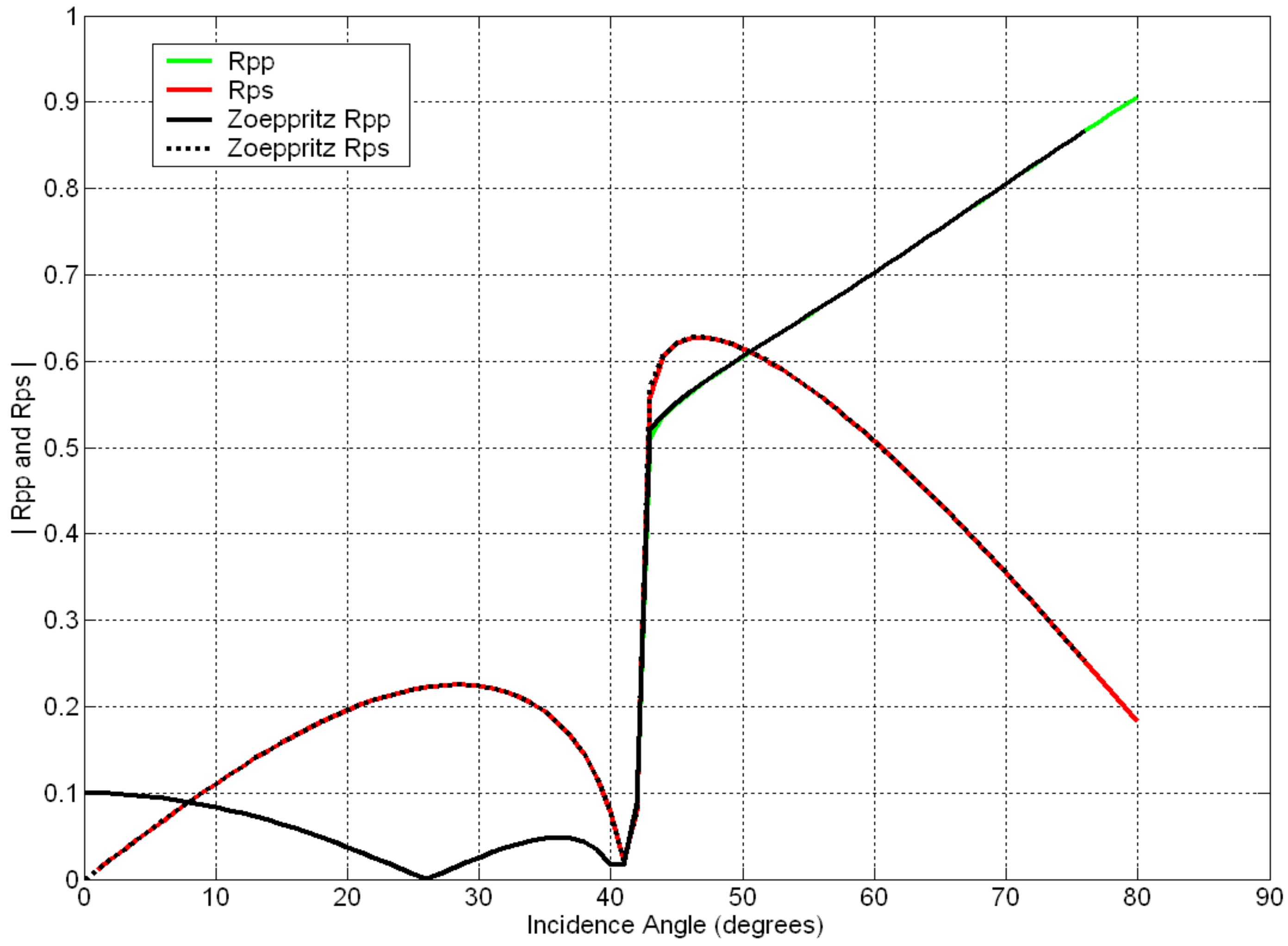

Plane-Wave Class 1 Elastic Reflection Coefficient

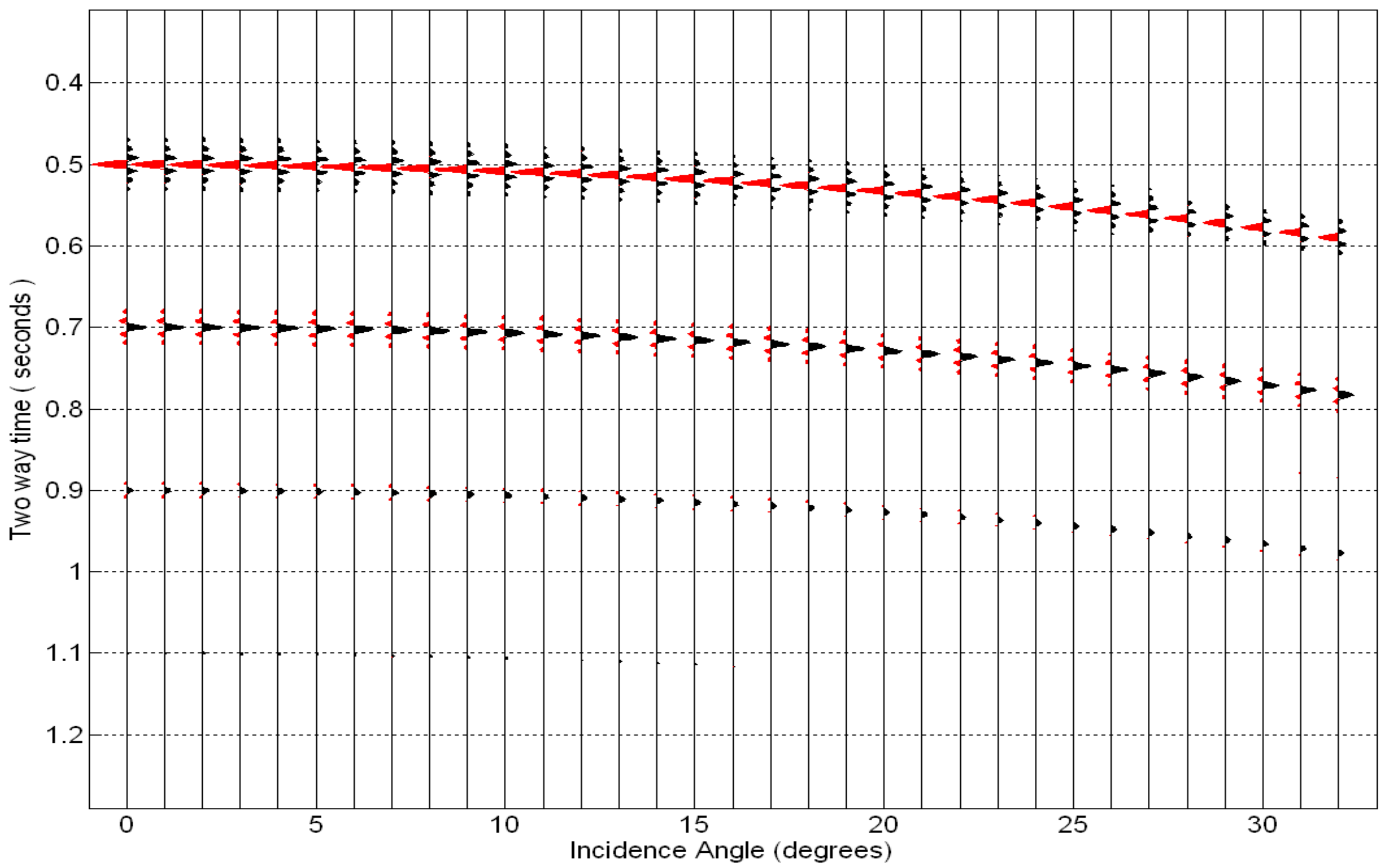

P-Wave Response of a 100 m Reservoir (top at 500 m)

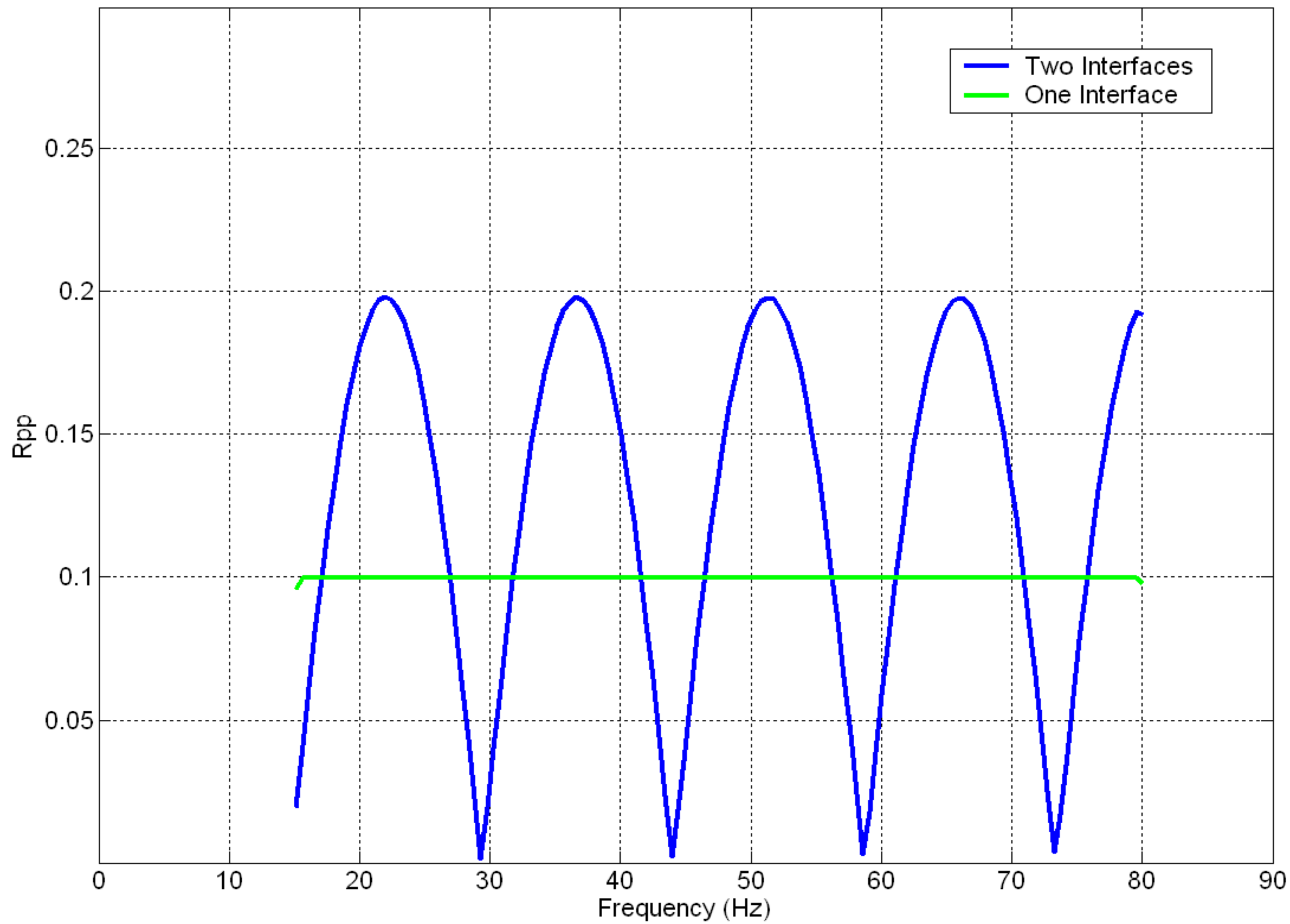

Plane-Wave $R_{pp}(\omega)$ (vertical incidence, 100 m reservoir)

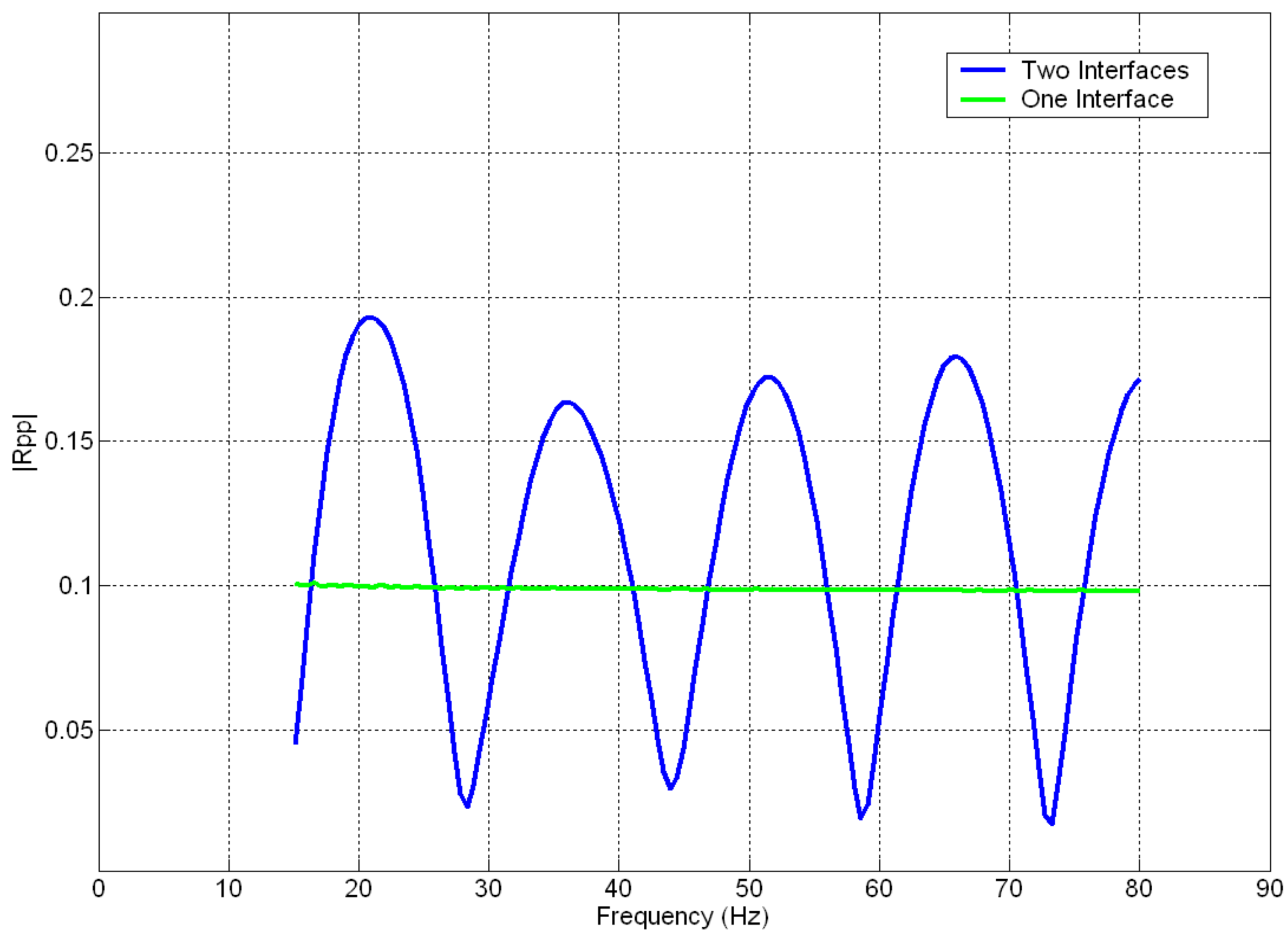

Spher.-Wave $R_{pp}(\omega)$ (vertical incidence, 100 m reservoir)

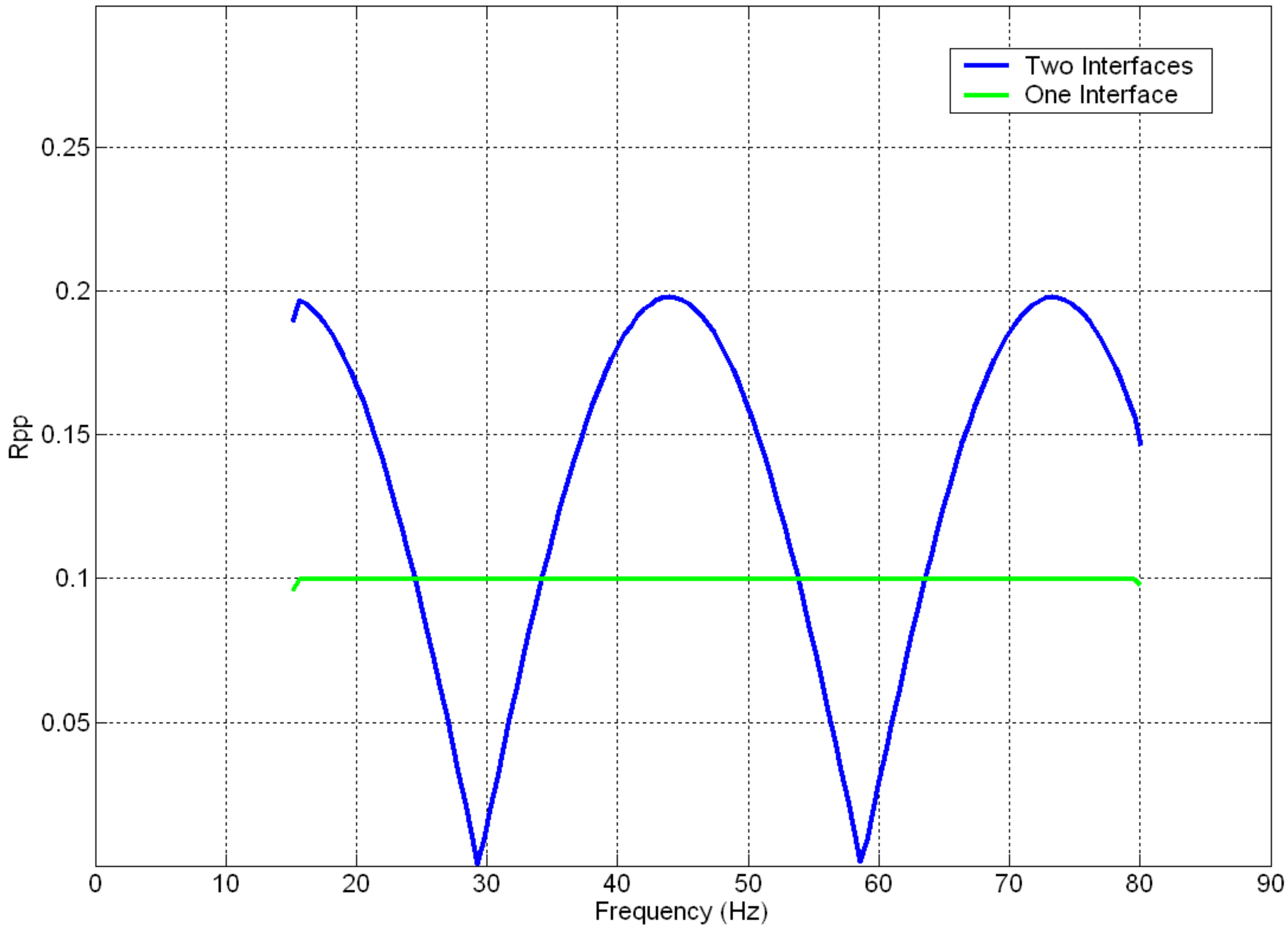

Plane-Wave $R_{pp}(\omega)$ (vertical incidence, 50 m reservoir)

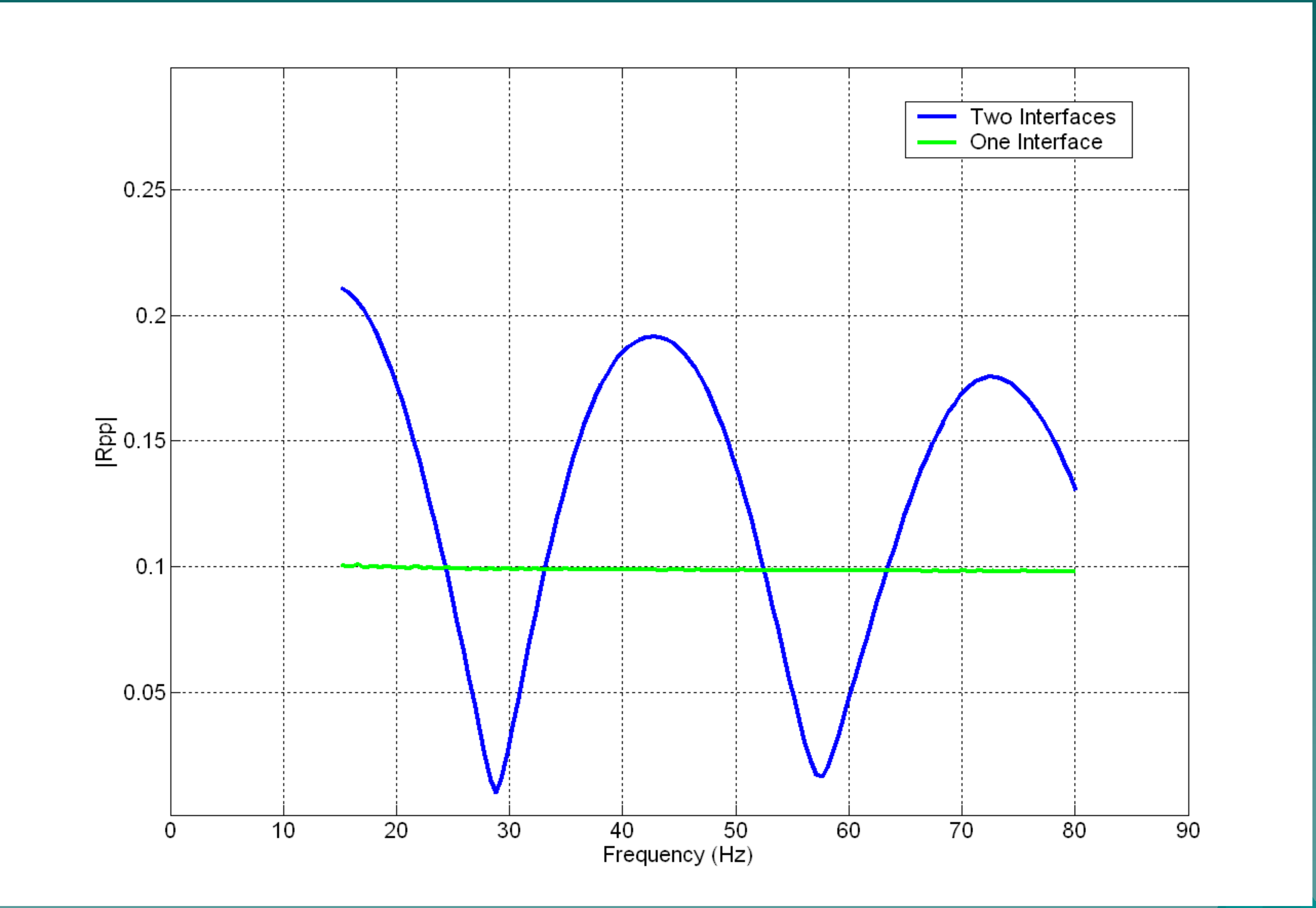

Spher.-Wave $R_{pp}(\omega)$ (vertical incidence, 50 m reservoir)

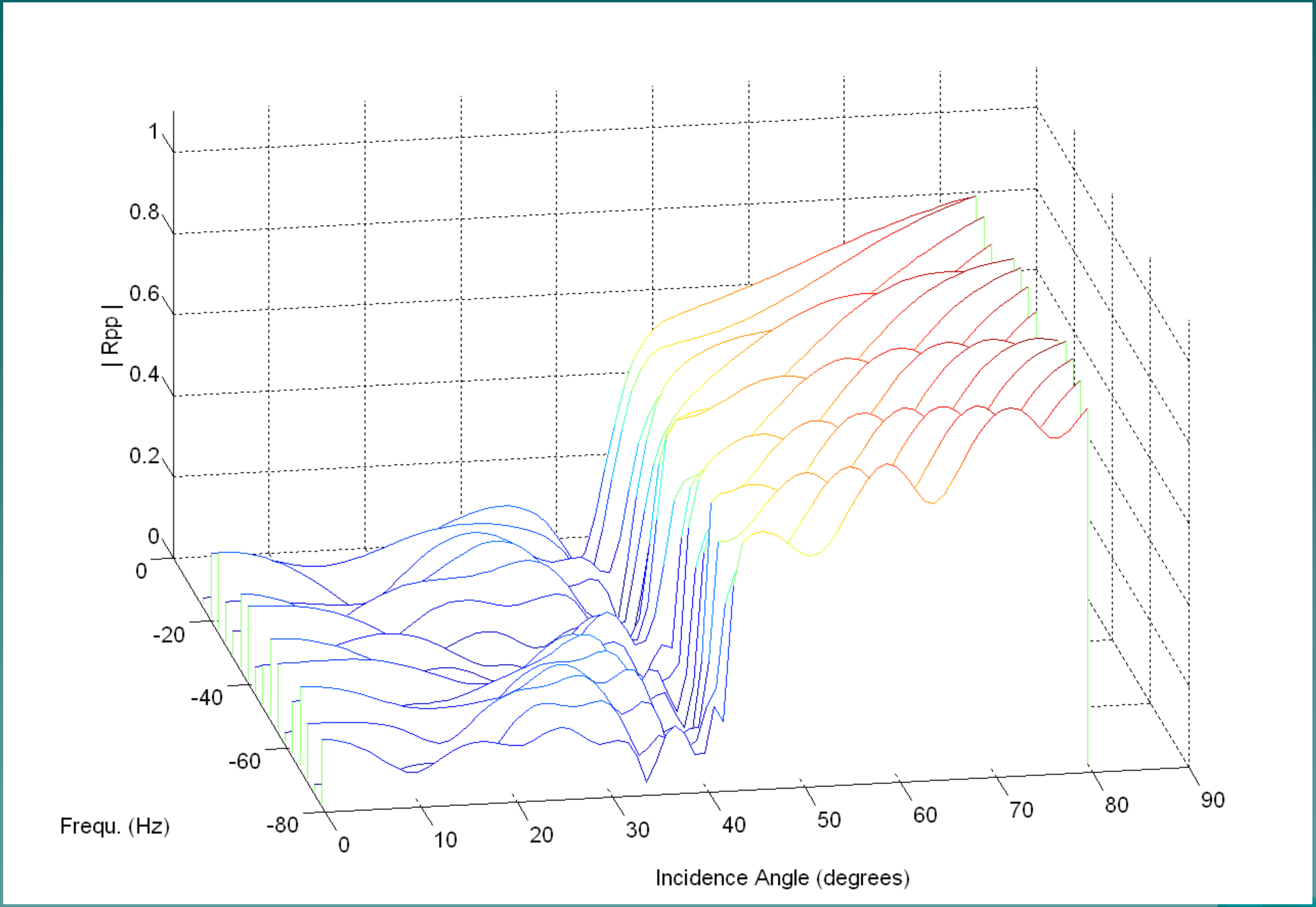

Plane-Wave $R_{pp}(\omega)$ (100 m reservoir)

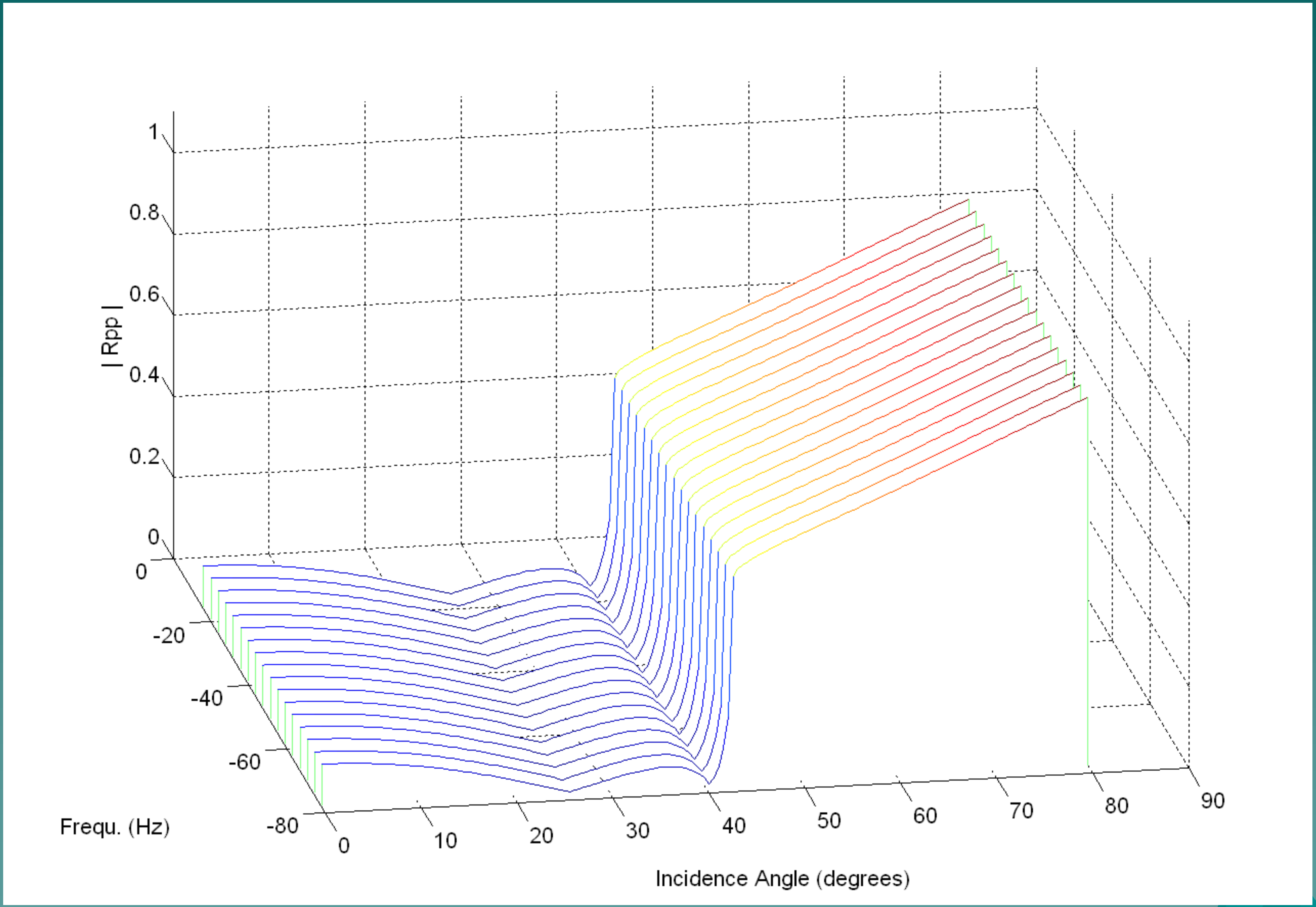

Plane-Wave $R_{pp}(\omega)$ (single interface)

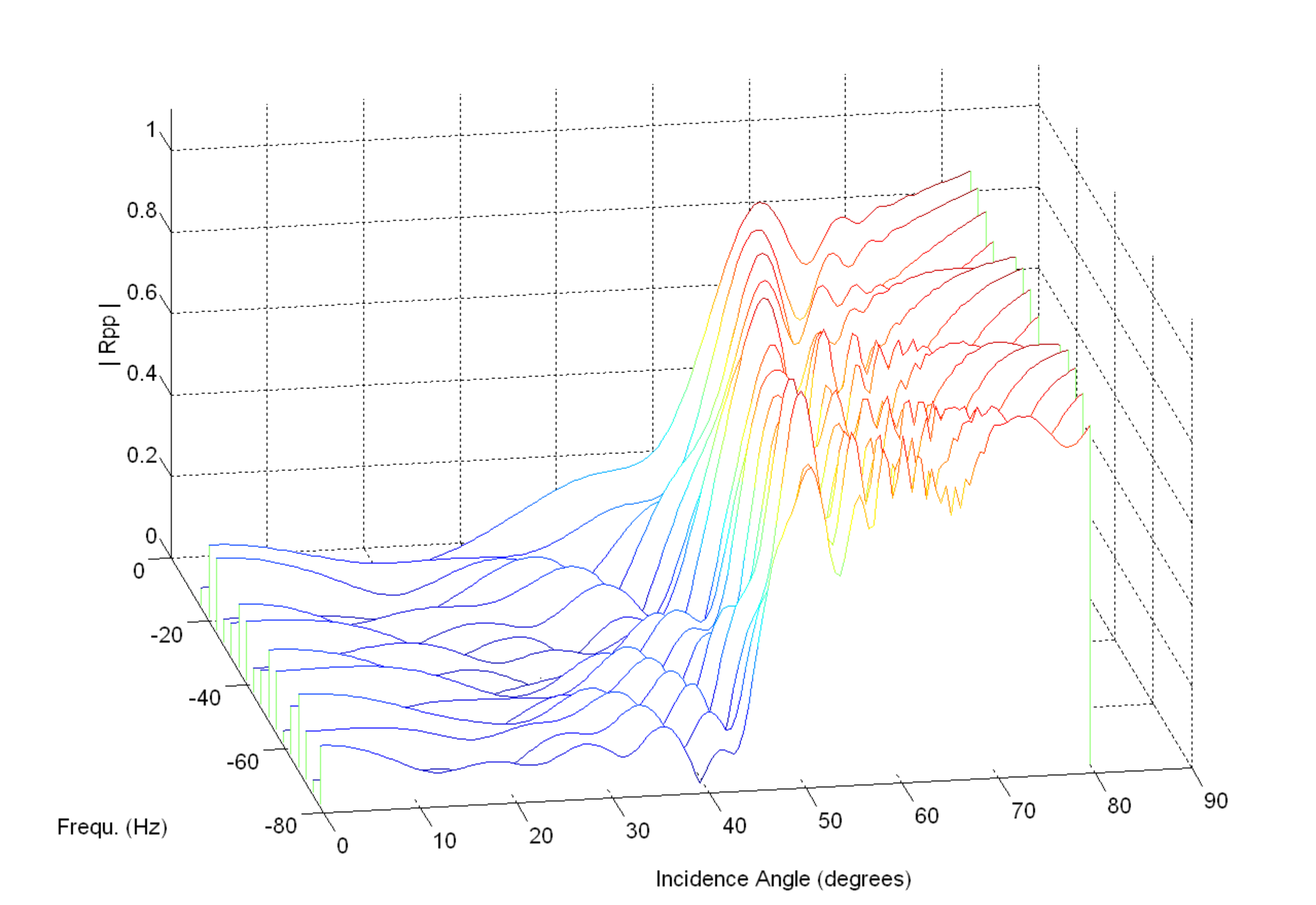

Spherical-Wave $R_{pp}(\omega)$ (100 m reservoir)

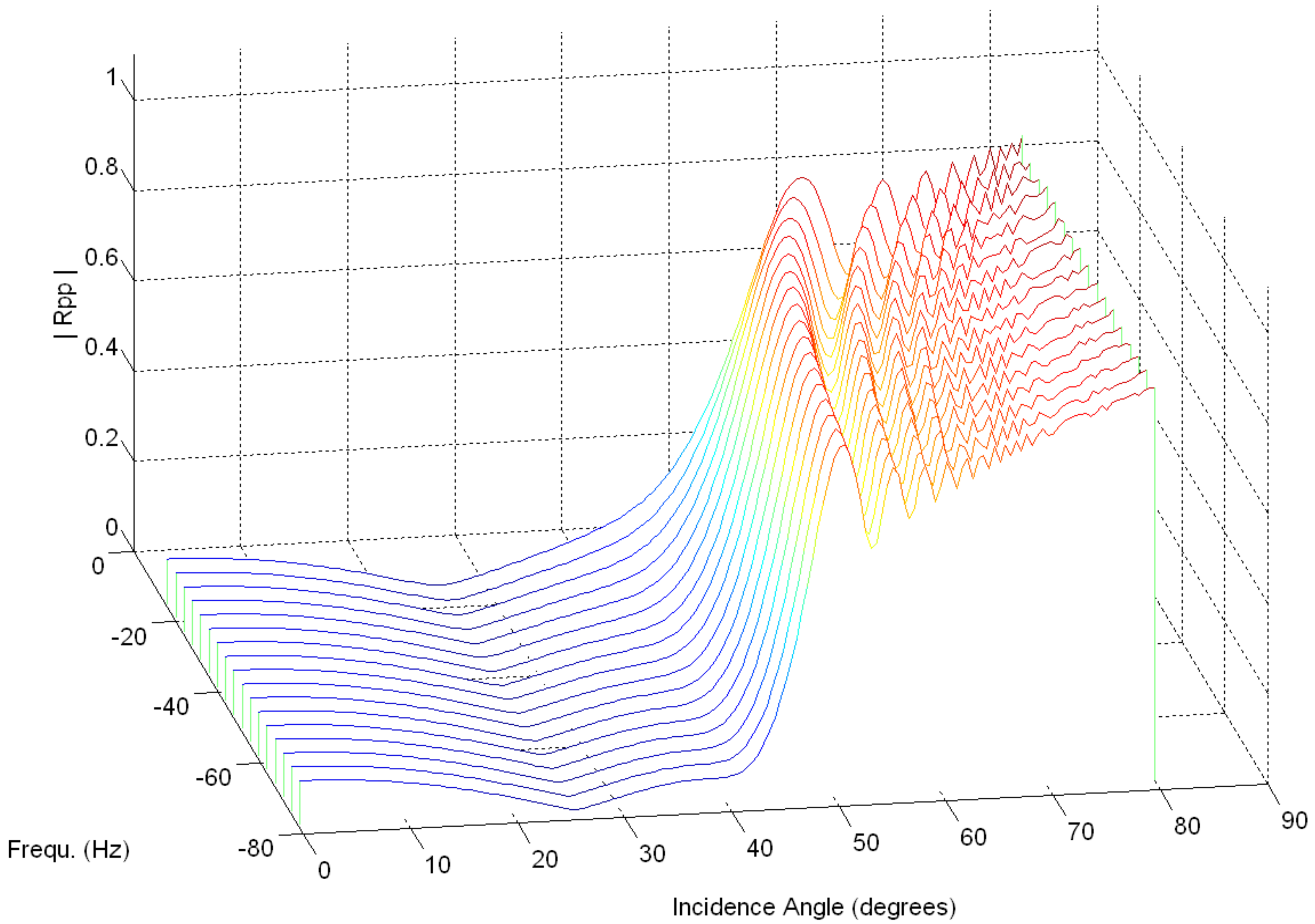

Spherical-Wave $R_{pp}(\omega)$ (single interface)

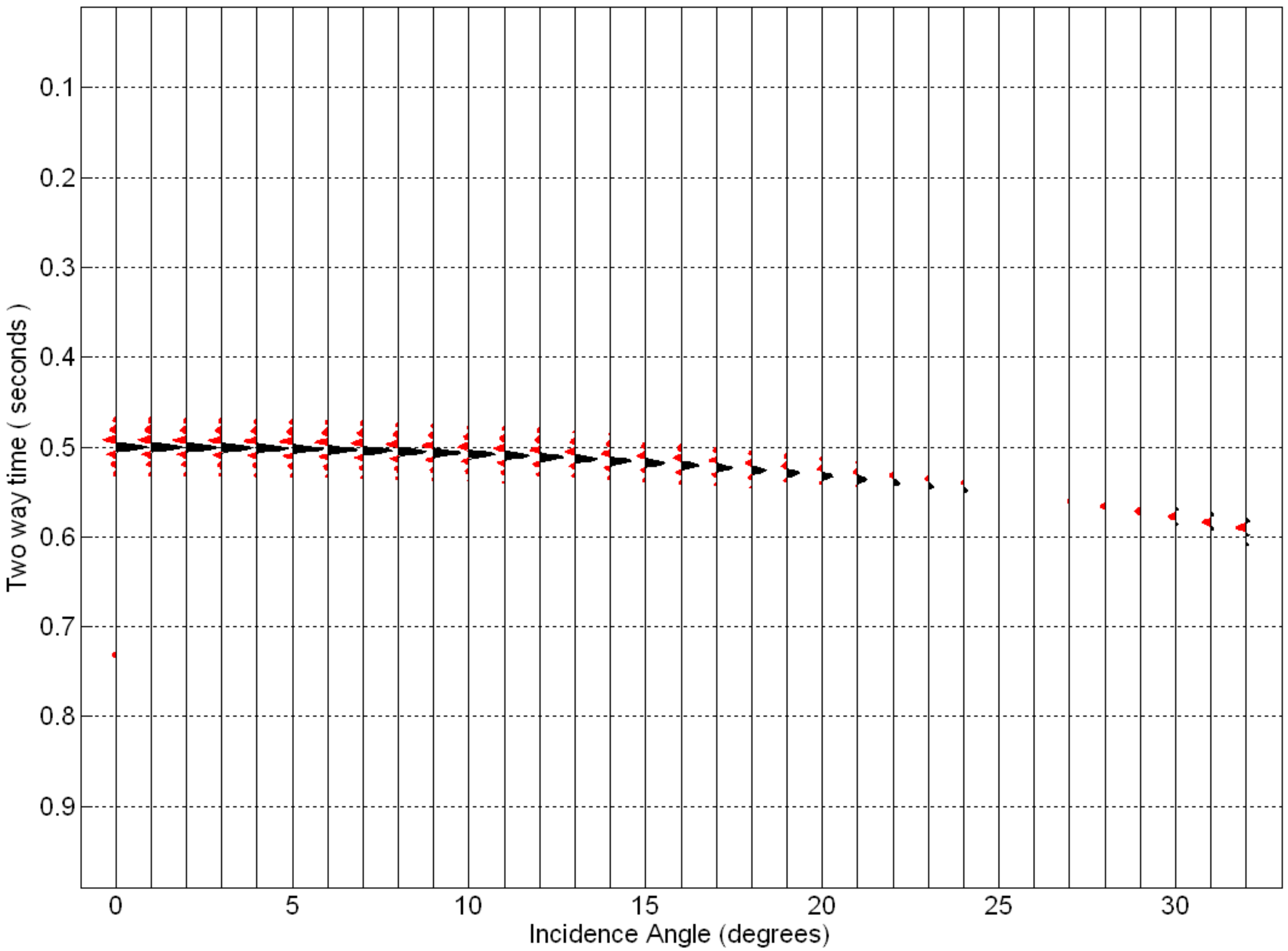

Spherical-Wave PP-Response (single reflector at 500m)

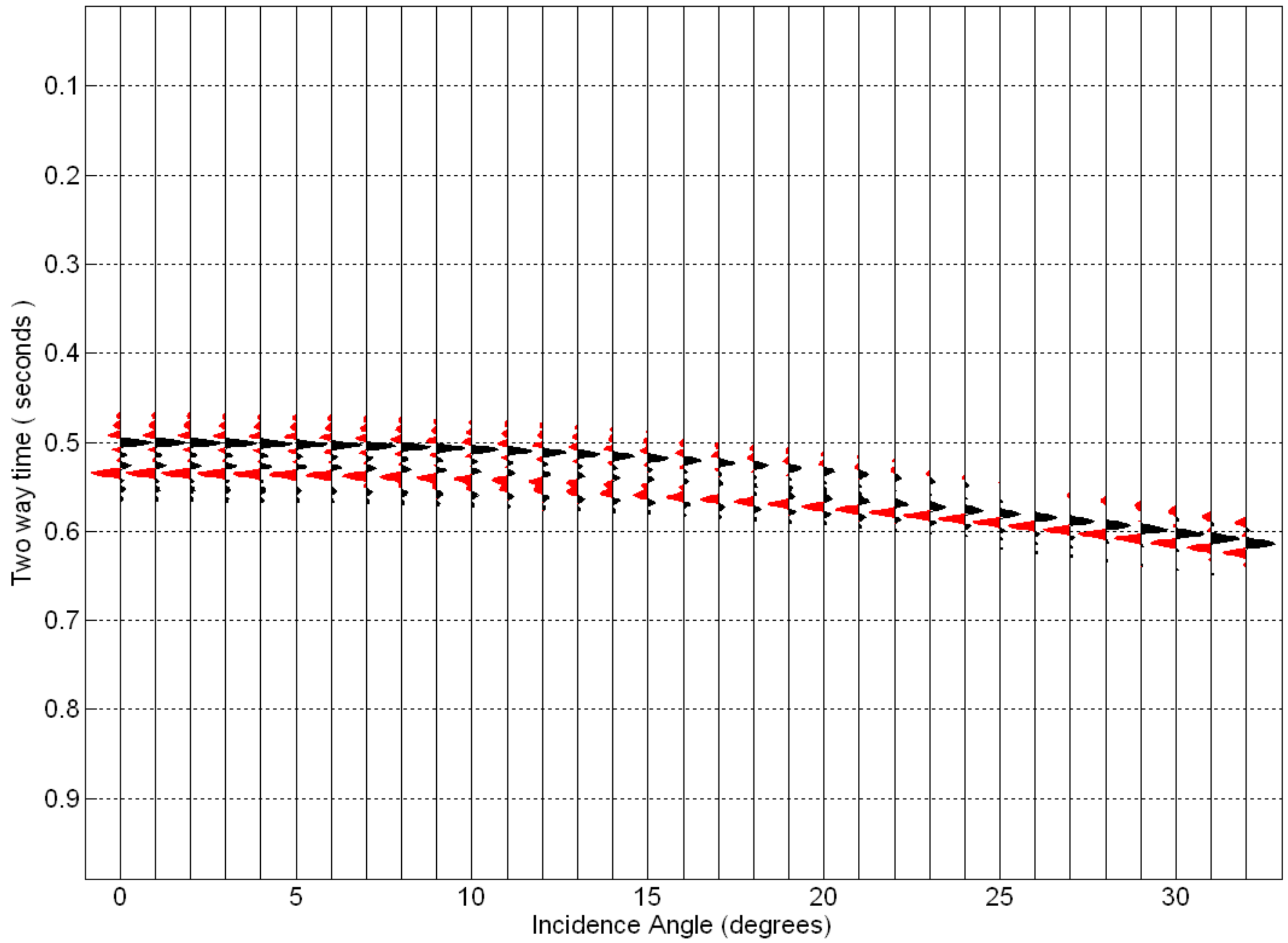

Spherical-Wave PP-Response (50 m reservoir)

Conclusions

- Reverberations and spherical spreading are modelled by the Ewing-method.
- Small-offset Class 1 AVO-responses show reservoir layer reverberations in the frequency-domain but at larger offsets the response is obscured.
- Time-domain responses show an amplitude build-up because of far-offset tuning.

Acknowledgements

Support by the CREWES team and its industrial sponsorship is gratefully acknowledged.
The author specifically would like to thank Professor E. Krebes for help with the theory.

Thank you for your attention.